

Glass-clad single-crystal germanium optical fiber

J. Ballato,^{1,*} T. Hawkins,¹ P. Foy,¹ B. Yazgan-Kokuoz,¹ R. Stolen,¹ C. McMillen,² N. K. Hon,³ B. Jalali,³ and R. Rice⁴

¹Center for Optical Materials Science and Engineering Technologies (COMSET)
School of Materials Science and Engineering, Clemson University, Clemson, SC 29631, USA

²Department of Chemistry, Clemson University, Clemson, SC 29631, USA

³Department of Electrical Engineering, UCLA, Los Angeles, CA 29631, USA

⁴Northrop Grumman Space Technology, Redondo Beach, CA 90278, USA

*jballat@clemson.edu

Abstract: Long lengths (250 meters) of a flexible 150 μm diameter glass-clad optical fiber containing a 15 μm diameter crystalline and phase-pure germanium core was fabricated using conventional optical fiber draw techniques. X-ray diffraction and spontaneous Raman scattering measurements showed the core to be very highly crystalline germanium with no observed secondary phases. Elemental analysis confirmed a very well-defined core-clad interface with a step-profile in composition and nominally 4 weight-percent oxygen having diffused into the germanium core from the glass cladding. For this proof-of-concept fiber, polycrystalline n-type germanium of unknown dopant concentration was used. The measured infrared transparency of the starting material was poor and, as a likely outcome, the attenuation of the resultant fiber was too high to be measured. However, the larger Raman cross-section, infrared and terahertz transparency of germanium over silicon should make these fibers of significant value for fiber-based mid- to long-wave infrared and terahertz waveguides and Raman-shifted infrared light sources once high-purity, high-resistivity germanium is employed.

©2009 Optical Society of America

OCIS codes: (160.4760) Optical properties; (160.2290) Fiber materials; (160.4330) Nonlinear optical materials; (160.6000) Semiconductor materials; (060.2290) Fiber materials; (060.2310) Fiber optics; (060.2390) Fiber optics, infrared; (060.4370) Nonlinear optics, fibers; (190.0190) Nonlinear optics; (190.4370) Nonlinear optics, fibers; (190.5650) Raman effect

References and Links

1. B. Jalali, V. Raghunathan, D. Dimitropoulos, and O. Boyraz, "Raman-based silicon photonics," *IEEE J. Sel. Top. Quantum Electron.* **12**(3), 412–421 (2006).
2. V. Raghunathan, D. Borlaug, R. Rice, and B. Jalali, "Demonstration of a mid-infrared silicon Raman amplifier," *Opt. Express* **15**(22), 14355–14362 (2007).
3. P. J. Sazio, A. Amezcua-Correa, C. E. Finlayson, J. R. Hayes, T. J. Scheidmantel, N. F. Baril, B. R. Jackson, D. J. Won, F. Zhang, E. R. Margine, V. Gopalan, V. H. Crespi, and J. V. Badding, "Microstructured optical fibers as high-pressure microfluidic reactors," *Science* **311**(5767), 1583–1586 (2006).
4. D.-J. Won, M. Ramirez, H. Kang, V. Gopalan, N. Baril, J. Calkins, J. Badding, and P. Sazio, "All-optical modulation of laser light in amorphous silicon-filled microstructured optical fibers," *Appl. Phys. Lett.* **91**(16), 161112 (2007).
5. B. Jackson, P. Sazio, and J. Badding, "Single crystal semiconductor wires integrated into microstructured optical fibers," *Adv. Mater.* **20**(6), 1135–1140 (2008).
6. J. Ballato, T. Hawkins, P. Foy, R. Stolen, B. Kokuoz, M. Ellison, C. McMillen, J. Reppert, A. M. Rao, M. Daw, S. Sharma, R. Shori, O. Stafsudd, R. R. Rice, and D. R. Powers, "Silicon optical fiber," *Opt. Express* **16**(23), 18675–18683 (2008).
7. J. Parker, D. Feldman, and M. Ashkin, "Raman scattering by silicon and germanium," *Phys. Rev.* **155**(3), 712–714 (1967).
8. J. Ballato, and E. Snitzer, "Fabrication of fibers with high rare-earth concentrations for Faraday isolator applications," *Appl. Opt.* **34**(30), 6848–6854 (1995).
9. J. Ballato, T. Hawkins, P. Foy, B. Kokuoz, R. Stolen, C. McMillen, M. Daw, Z. Su, T. Tritt, M. Dubinskii, J. Zhang, T. Sanamyan, and M. J. Matthewson, "On the Fabrication of All-Glass Optical Fibers from Crystals," *J. Appl. Phys.* **105**(5), 053110 (2009).
10. G. M. Sheldrick, "A short history of SHELX," *Acta Crystallogr. A* **64**(1), 112–122 (2008).

11. C. F. Macrae, P. R. Edgington, P. McCabe, E. Pidcock, G. P. Shields, R. Taylor, M. Towler, and J. van de Streek, "Mercury: visualization and analysis of crystal structures," *J. Appl. Cryst.* **39**(3), 453–457 (2006).
 12. J. Donohue, *The Structure of the Elements*, Wiley, New York, (1974).
 13. J. Scott, "Raman spectrum of GeO₂," *Phys. Rev. B* **1**(8), 3488–3493 (1970).
 14. R. Stolen, "Fundamentals of Raman Amplification in Fibers," in *Raman Amplifiers for Telecommunication I*, M. Islam, editor, Springer (New York, 2004); see Appendix A2.5.
 15. B. Frey, D. Leviton, and T. Madison, "Temperature-dependent refractive index of silicon and germanium," *Proc. SPIE* **6273**, 62732J (2006).
 16. J. Pankove, and P. Aigrain, "Optical absorption of arsenic-doped degenerate germanium," *Phys. Rev.* **126**(3), 956–962 (1962).
 17. E. Capron, and O. Brill, "Absorption coefficient as a function of resistance for optical germanium at 10.6 μm ," *Appl. Opt.* **12**(3), 569–572 (1973).
 18. P. Bishop, and A. Gibson, "Absorption coefficient of germanium at 10.6 μm ," *Appl. Opt.* **12**(11), 2549–2550 (1973).
-

1. Introduction

Continued rapid advances in silicon-based photonics have generated intense interest in the eventual integration of electronics and photonics [1,2]. The extension of silicon photonics from a planar waveguide platform to an optical fiber-based technology would be a significant progression in this emerging field. This would definitely enable additional functionalities and capabilities in silicon photonics. There have been several important steps towards semiconductor core optical fiber [3–5]. Recently, highly crystalline silicon core optical fibers were produced for the first time using commercially-scalable fiber draw techniques [6]. While those fibers exhibited attenuation values in the mid-infrared (~ 4 dB/m) that are acceptable for selected applications, atomic diffusion arising from the high processing temperatures (~ 2000 °C) led to detrimental effects on oxygen content that could negate the likelihood of single-mode fibers in the infrared.

In the present work, germanium (Ge) was considered for several reasons. Firstly, Ge melts at nearly 500K below silicon and so diffusion – a thermally activated process – would be greatly reduced. Further, relative to Si, Ge has extended infrared transparency and higher Raman gain making it a very intriguing core material for new infrared transmission fibers and fiber-based light sources [7].

The purpose of this report is to describe the fabrication and physical properties of glass-clad, flexible, and highly-crystalline Ge core optical fiber that was fabricated using a molten core approach coupled with commercially-accepted fiber production methods [6–9]. Details of the optical characteristics will be addressed in a sequel.

2. Experimental

A 3 mm rod was core-drilled out of a slab of 99.99% pure, n-type, arsenic-doped Ge of unknown dopant concentration (Lattice Materials, Bozeman, MT). This rod was sleeved into a glass tube having an inner diameter slightly larger than 3 mm and outer diameter of 30 mm. This cladding tube had been pre-drawn in order to collapse and seal one end of the tube so that the Ge core, which is molten during the fiber draw, was confined.

Fibers were drawn at Clemson University using the Heathway draw tower at approximately 1000°C. At this temperature, the Ge core is above its melting temperature (938°C) and the liquid is encapsulated by the softened glass cladding. This approach is similar to what has been used previously to develop fibers possessing traditionally non-fiberizable materials [6,9]. Approximately 250 meters of 150 μm diameter fiber was drawn, which yielded a core size of 15 μm . The fibers were coated to an outer diameter of about 240 μm using a UV-curable acrylate coating and collected on a 75 mm diameter spool, which attests to its flexibility.

The cross-section of the fibers was imaged using electron microscopy. Electron microscopy was performed using a Hitachi 3400N scanning electron microscope (SEM). The electron microscope was operated at 20 or 30 kV and 10 mm working distance under variable pressure. Elemental analysis via energy dispersive x-ray spectroscopy (EDX) was used to

examine the distribution of elements across the core/clad interface. Elemental compositions were measured at several locations traversing the core.

Single crystal x-ray diffraction was performed at room temperature on a 1 mm length of fiber using a Rigaku AFC8S diffractometer equipped with graphite monochromated Mo K α radiation and a Mercury CCD area detector. This 1 mm section was randomly selected from the 250 meters of drawn fiber. A total of 480 diffraction images were collected and used for subsequent structure determination and refinement using the *SHELXTL* software package [10]. Powder diffraction data were simulated from the final refined single crystal data using the *Mercury CSD* software package (version 2.0) [11]. This was done to provide a more “graphical” representation of the crystallinity.

Raman spectra were collected on both the Ge starting rods and the drawn fibers using a R-3000 series instrument (Raman Systems Inc.) with a 100 micron spot size at 20 mW of power at 785 nm wavelength excitation.

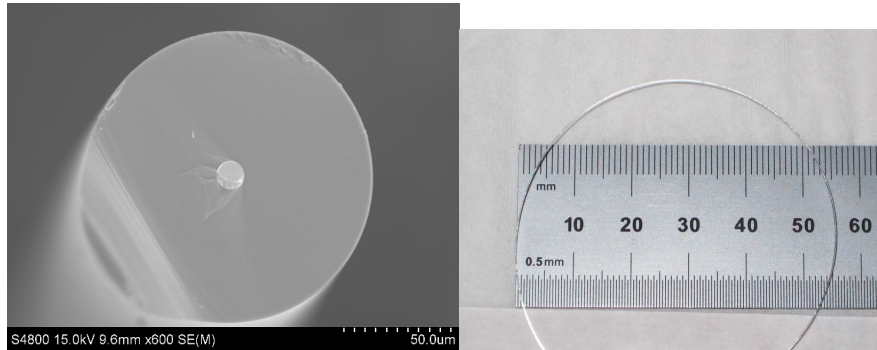


Fig. 1. [Left] Scanning electron micrograph of the fiber showing the central germanium core and the glass cladding (polymeric coating removed). [Right] Photograph of the coated fiber arranged into a circle of approximately 28 mm radius indicating its flexibility.

3. Results and Discussion

Figure 1 provides electron and optical images of the Ge core fiber. Figure 1 [left] is a scanning electron microscope image of the fiber after the polymer coating was removed. Clearly observed is a core of circular cross section and diameter of about 15 μm and no apparent interfacial irregularities at the core/clad boundary. Figure 1 [right] is an optical micrograph showing the flexibility of the (polymer coated) fiber.

Single crystal x-ray axial photographs were first used to verify the crystallinity of a selected region of the fiber. The reflection profiles of these axial photographs indicated the presence of only one crystal orientation within the beam diameter (0.8 mm). Given the perceived single crystallinity of this region, a full data set was collected and a very low final R-factor (0.0179) was obtained from this data, as would be expected from a monocrystalline sample. This structure determination produced a unit cell parameter of 5.6675 \AA , which is slightly higher than other experimentally measured values of about 5.657 \AA ; this latter being a compilation of data reported over the years from 1922 to 1968 [12]. However, since the doping concentration in the starting rod is not known, the influence of the arsenic, or other dopants, on the resultant lattice parameter cannot be estimated. The slightly larger unit cell parameter could be due to the dopants, the oxygen content (discussed below), or residual strain arising from thermal expansion differences with the cladding glass. Figure 2 provides a more conventional two-theta diffraction pattern simulated from the directly measured single crystal diffraction data. There is generally good agreement between the peak positions and intensities of the simulated pattern versus those indexed in the JCPDS database, with the slight shift to lower two-theta values in the observed data attributable to the higher lattice parameter.

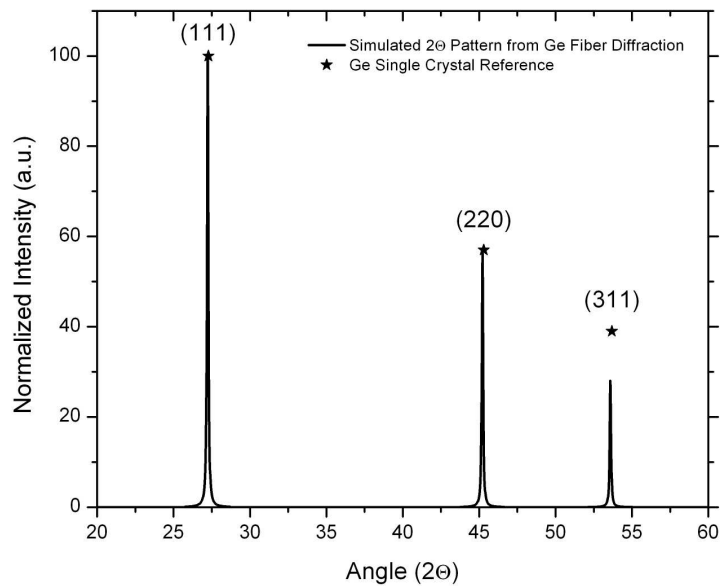


Fig. 2. Normalized intensity versus two-theta angle x-ray diffraction pattern computed from the refined single crystal diffraction data. The stars represent the normalized intensities for those noted crystallographic planes.

Elemental analysis was performed on a cross-section of the fiber in order to determine the extent to which the diffusion occurs during the draw between the softened glass cladding and the molten Ge core. Figure 3 provides the compositional profile along a line crossing the full diameter of the core as well as the interface into the cladding. Error bars representing a 95% confidence interval are included but might not be resolvable on the graph as they are smaller than the graphical size of the data point.

Several observations can be made. First, the core is principally Ge with about 4 weight-percent oxygen diffusing in from the oxide glass cladding during the draw. This is considerably less oxygen than was the case with the silicon fiber [6], which was approximately 17 weight-percent, and is due to the reduced processing temperature used here even though the diffusion distance is considerably shorter (approximately 75 μm core radius in the case of the silicon but only about 7-8 μm – the radius of the circularly symmetric core – in this case of Ge). Since diffusion is a thermally-activated process, a lowering of the processing temperature favors a reduced degree of diffusion.

Second, the core compositional profile is flat. This is because the core is molten during the draw and fluid melt homogenizes during the transition from larger preform to smaller fiber. This feature was also observed in the silicon core optical fiber [6]. Additionally, the interface is well-defined, to the approximately 1 μm spatial resolution of the EDX measurement, and defines a more step-like refractive index profile than is observed in conventional glass-core glass-clad optical fibers.

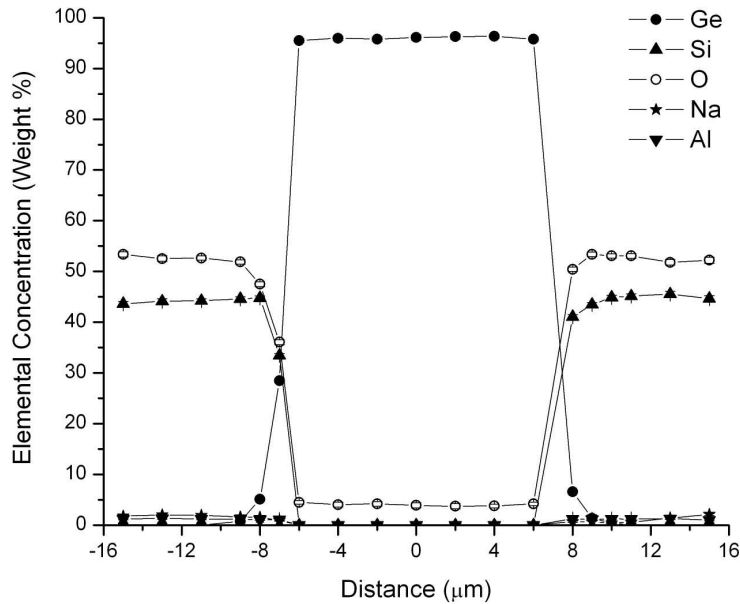


Fig. 3. Elemental analysis of the glass-clad, germanium core optical fiber.

Figure 4 provides a comparison of the spontaneous Raman scattering spectrum for the core of the Ge fiber relative to the starting Ge rod from which the fiber was drawn. As can be seen, there is a minor shift in the peak position and broadening of the line-width of the Ge crystal in the fiber core relative to that of the starting crystal rod. However, the significant similarities between starting crystal and core of the drawn fiber further imply a high degree of crystallinity and phase-purity. It is important to note that Ge-O vibrations at about 800 cm^{-1} [13] are not observed. This might be attributable to the fact that the line-strength for the Ge-Ge vibrations are much stronger than those for the Ge-O, hence possibly are over-shadowed given the measured 4 weight-percent oxygen content. The inability to observe oxide-related impurities by Raman scattering was also the case of the silicon optical fiber [6].

The Raman cross-section and gain coefficient for Ge has not been studied as extensively as it has in Si. An initial estimation for the relative intensity of Ge with respect to silicon suggested that Ge had a higher scattering intensity than silicon by a factor between 1.2 and 2, although corrections for the refractive index and penetration depth were not made in that work [7]. A simple model for Raman gain, based on polarizability, through the refractive index (n), yields a $(n^2-1)^2/n^2$ proportionality [14]. Given the refractive index as a function of wavelength [15] the ratio of Raman gain for Ge would be between 45 and 50% higher than silicon over the 2 to 5 μm wavelength range.

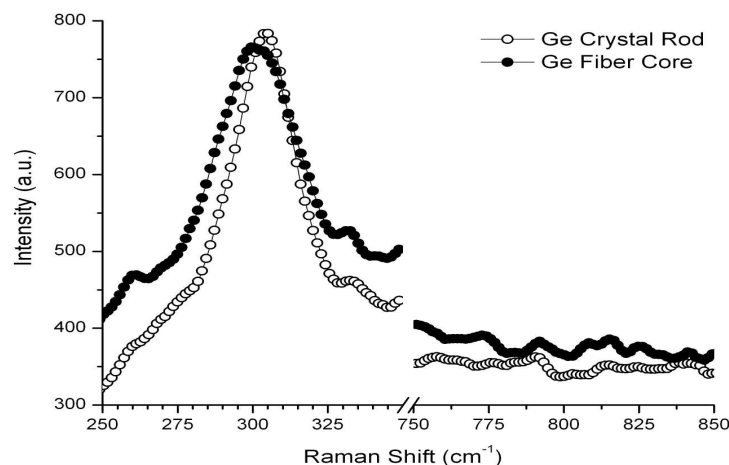


Fig. 4. Spontaneous Raman scattering spectra of a single crystalline germanium rod and the germanium core of a glass-clad fiber.

A number of attenuation measurements of the starting rod and the fiber were attempted with unsuccessful results. The transmission through the core rod was uniformly weak ($< 10\%$ over 1 cm thickness) over the range from 2.5 to 20 μm indicating significant broadband loss in the raw material. The raw material is specified by the commercial source to be arsenic-doped n-type Ge although the doping level and concentration of other impurities is unknown. For microelectronic applications, the typical doping levels would have virtually no impact on the crystalline structure but could render the Ge sufficiently conductive to an extent that would negate infrared transparency over practical lengths. The attenuation of arsenic-doped Ge is known to be quite high over the infrared spectral range of interest [16]. Therefore, the presence of mid-gap levels, either impurities or defects of some nature, in the starting material is conjectured to be the source of the poor transmission in the original core rod and, therefore, in the resultant fiber. Further, the influence of the oxygen or other species that diffused into the core from the cladding glass on the fiber attenuation also has not yet been determined but is a focus of on-going studies.

Though far from optimized, the single crystal silicon core optical fibers demonstrated reasonably low optical attenuation in the mid-infrared, about 4.3 dB/m at 3 microns wavelength [6]. With the present Ge core fibers, losses are much higher, even though the appearance of the fibers and their physical property measurements are comparatively quite excellent.

There are several strategies to mitigate attenuation that will follow in future work. Work is presently underway to identify and eliminate the origin of the losses in the drawn Ge core fiber. Future fiber draws will employ the highest-purity and lowest-conductivity Ge material available since the absorption coefficient of Ge, particularly in the 3 – 10 μm spectral range is known to be primarily dependent on carrier concentration [17,18].

4. Conclusions

To the best of our knowledge, this constitutes the first report of long lengths of highly crystalline semiconductor core fibers. More specifically, 250 meters of 150 μm diameter glass-clad optical fiber were fabricated that possessed a 15 μm Ge core. X-ray diffraction and Raman spectroscopy confirmed the core to be phase-pure, highly crystalline, and with a nominal amount of oxygen that diffuses into the core from the cladding during the draw process. Presently, absorption levels in both the starting crystal rod and in the resultant fiber were too high to measure infrared transparency. However, it is reasonable to expect, given the

otherwise high quality of this proof-of-concept fiber, that fibers drawn from high purity precursors would yield practical results.

Acknowledgments

The authors wish to acknowledge financial support from the State of South Carolina and Northrop Grumman Space Technology.